Supporting Information for:

Perylene Monoimide and Naphthalene-Annulated [3,3,3]propellanes: Synthesis and Device applications

Lingling Lv,[a] Wenda Sun,[b] Zhenmei Jia,[a] Guowei Zhang,[a] Fuzhi Wang,[b] Zhanao Tan*[a,b] and Lei Zhang*[a]

Table of contents

1. Characterization of the compounds

^{1}H NMR and ^{13}C NMR spectra were recorded in deuterated solvents on Bruker ADVANCE 400 NMR Spectrometer and Bruker FOURIER 100 NMR Spectrometer. ^{1}H NMR chemical shifts were reported in ppm downfieldfrom tetramethylsilane (TMS) reference using the residual protonated solvent as aninternal standard. High resolution mass spectra (HR- MALDI-TOF-MS) were determined on a Bruker BIFLEX III Mass Spectrometer.

2. Thermal stability of the compounds

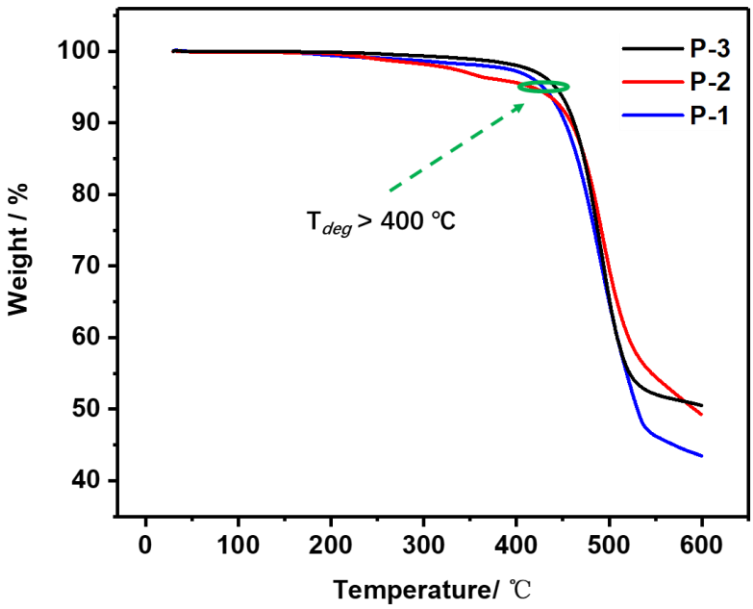

Figure S1. TGA curves of **P-1**, **P-2** and **P-3**.

3. Computational Methology

The density functional theory (DFT) calculations were performed with the Gaussian 09 Rev. E.01 employing the 6-31G(d, p) basis set. For all of the molecules we present at least the 60 lowest-energy roots determined by the TD-DFT calculations. Considering the alkyl chains on the imide positions has negligible effect on the final structural and electronic properties of these compounds, we chose methyl substituents instead of 2-decyltetradecyl on the imide positions for better view of their structures. TD-DFT singlet excitation energies E, excitation wavelengths λ, oscillator strengths f > 0.01, and orbital contributions at the optimized S_0 ground state geometry in chloroform at B3LYP/6-31G(d, p) level.

Table S1. Pictorial representations of selected frontier molecular orbitals of **P-1**, and **P-2** as determined at the B3LYP/6-31G(d, p) level of theory.

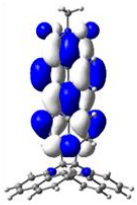	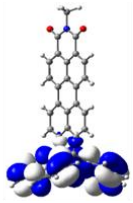	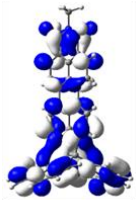	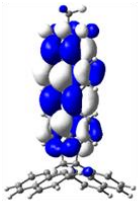	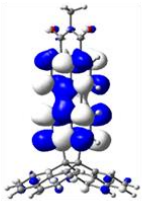
LUMO=-2.71 eV	LUMO+1=-1.41 eV	LUMO+2=-1.16 eV	LUMO+3=-1.02 eV	LUMO+4=-0.88 eV
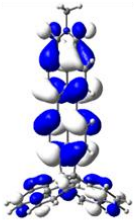	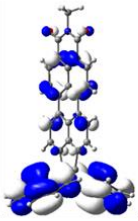	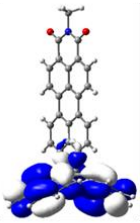	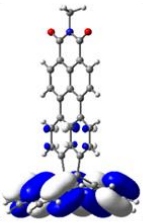	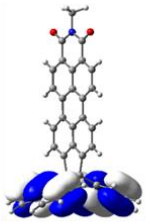
HOMO=-5.32 eV	HOMO-1=-5.84 eV	HOMO-2=-6.12 eV	HOMO-3=-6.77eV	HOMO-4=-6.85 eV
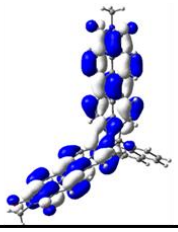	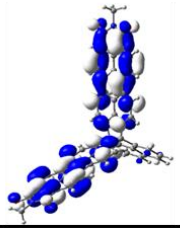	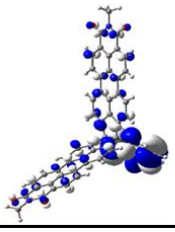	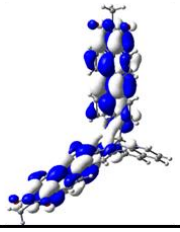	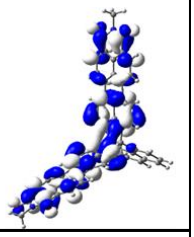
LUMO=-2.95 eV	LUMO+1=-2.78 eV	LUMO+2=-1.49 eV	LUMO+3=-1.25eV	LUMO+4=-1.20 eV
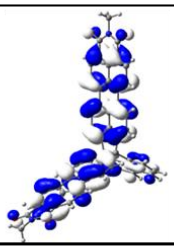	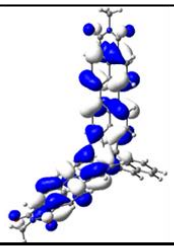	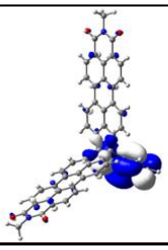	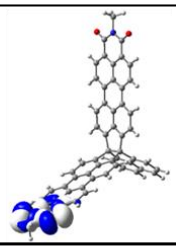	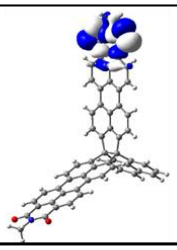
HOMO=-5.42 eV	HOMO-1=-5.66 eV	HOMO-2=-6.20 eV	HOMO-3=-6.99eV	HOMO-4=-6.99 eV

1) compound P-1

Excited State 1: Singlet-A 2.4224 eV 511.83 nm f=0.6500 <S**2>=0.000
157 ->159 -0.15510
158 ->159 0.68874

Excited State 2: Singlet-A 2.7798 eV 446.01 nm f=0.1181 <S**2>=0.000
157 ->159 0.68709
158 ->159 0.15404

Excited State 3: Singlet-A 2.9906 eV 414.58 nm f=0.0111 <S**2>=0.000
156 ->159 0.70418

Excited State 5: Singlet-A 3.4750 eV 356.78 nm f=0.0309 <S**2>=0.000

158 ->160 0.70424

Excited State 12: Singlet-A 3.8019 eV 326.11 nm f=0.0121 <S**2>=0.000
150 ->159 0.53309
152 ->159 -0.21479
158 ->163 0.28033
158 ->166 0.18782
158 ->167 0.12638

Excited State 14: Singlet-A 3.9502 eV 313.87 nm f=0.1239 <S**2>=0.000
157 ->160 0.69728

Excited State 15: Singlet-A 3.9626 eV 312.89 nm f=0.0156 <S**2>=0.000
148 ->159 0.43686
149 ->159 -0.19747
152 ->159 0.30476
158 ->163 -0.28685
158 ->164 -0.10800
158 ->166 0.20265
158 ->167 0.10462

Excited State 17: Singlet-A 4.1525 eV 298.58 nm f=0.0127 <S**2>=0.000
149 ->159 0.17281
156 ->160 0.51661
157 ->161 0.40506
158 ->164 -0.14780

Excited State 22: Singlet-A 4.3632 eV 284.16 nm f=0.0590 <S**2>=0.000
149 ->159 -0.15899
156 ->160 0.45384
157 ->161 -0.43989
158 ->164 0.19967

Excited State 23: Singlet-A 4.4361 eV 279.49 nm f=0.0100 <S**2>=0.000
148 ->159 0.18657
154 ->160 0.26576
155 ->161 -0.12381
156 ->165 -0.18193
157 ->162 0.41043
157 ->163 0.14155
157 ->166 0.13364
157 ->167 -0.10845
158 ->163 0.10899
158 ->166 -0.24470

158 ->167 0.15517

Excited State 24: Singlet-A 4.4608 eV 277.94 nm f=0.0542 <S**2>=0.000
156 ->161 0.69076

Excited State 29: Singlet-A 4.6004 eV 269.51 nm f=0.0633 <S**2>=0.000
148 ->159 -0.23821
154 ->160 0.27046
156 ->165 -0.26507
157 ->163 -0.14632
157 ->167 -0.16279
158 ->166 0.43149

Excited State 33: Singlet-A 4.7541 eV 260.79 nm f=0.0598 <S**2>=0.000
148 ->159 -0.11536
150 ->159 -0.11894
156 ->165 0.21624
157 ->166 -0.10490
158 ->167 0.59083

Excited State 38: Singlet-A 5.0323 eV 246.38 nm f=0.0132 <S**2>=0.000
154 ->160 0.41509
155 ->161 0.53292
155 ->164 0.13339
157 ->166 -0.11306

2) compound P-2

Excited State 1: Singlet-A 2.2029 eV 562.82 nm f=0.6804 <S**2>=0.000
211 -> 212 0.70262
Excited State 2: Singlet-A 2.3342 eV 531.17 nm f=0.0105 <S**2>=0.000
210 -> 212 -0.42237
211 -> 213 0.56474

Excited State 3: Singlet-A 2.5963 eV 477.55 nm f=0.3513 <S**2>=0.000
210 -> 212 0.56197
211 -> 213 0.41766

Excited State 4: Singlet-A 2.5985 eV 477.14 nm f=0.5123 <S**2>=0.000
210 -> 213 0.70029

Excited State 5: Singlet-A 2.8270 eV 438.57 nm f=0.0443 <S**2>=0.000
209 -> 212 0.70263

Excited State 9:	Singlet-A	3.5166 eV	352.57 nm	f=0.0119	<S**2>=0.000	
211 -> 214	0.69644					
Excited State 20:	Singlet-A	3.7905 eV	327.09 nm	f=0.0133	<S**2>=0.000	
199 -> 212	0.39111					
200 -> 213	0.22653					
202 -> 212	0.12907					
203 -> 213	0.16037					
204 -> 212	-0.17222					
206 -> 213	-0.27475					
210 -> 218	-0.18048					
210 -> 222	-0.10611					
211 -> 219	-0.24931					
211 -> 223	-0.11221					
Excited State 23:	Singlet-A	3.8646 eV	320.82 nm	f=0.0209	<S**2>=0.000	
194 -> 213	-0.24969					
195 -> 212	-0.30703					
196 -> 212	0.34295					
197 -> 213	-0.25388					
199 -> 212	-0.19294					
206 -> 213	-0.19598					
210 -> 222	0.12219					
211 -> 223	0.10625					
Excited State 47:	Singlet-A	4.3363 eV	285.92 nm	f=0.1037	<S**2>=0.000	
198 -> 212	-0.13572					
201 -> 213	-0.11179					
209 -> 214	0.63504					
211 -> 220	0.16399					
Excited State 49:	Singlet-A	4.3730 eV	283.52 nm	f=0.0196	<S**2>=0.000	
195 -> 212	-0.11157					
197 -> 213	0.37524					
199 -> 212	-0.12414					
200 -> 213	-0.22572					
206 -> 214	-0.15682					
210 -> 215	-0.10496					
210 -> 218	-0.16969					
211 -> 219	-0.16468					
211 -> 221	-0.35388					
Excited State 54:	Singlet-A	4.5232 eV	274.11 nm	f=0.0140	<S**2>=0.000	

193 -> 212	-0.20635
206 -> 214	-0.30762
209 -> 215	-0.20038
209 -> 217	-0.18704
209 -> 219	0.32980
209 -> 221	-0.25011
211 -> 221	0.26847

Excited State 60: Singlet-A 4.6704 eV 265.47 nm f=0.0373 <S**2>=0.000

193 -> 213	0.56928
209 -> 217	-0.17017
209 -> 219	-0.16788
211 -> 223	-0.28778

4. OFET fabrication and characterization

Thin film fabrication: Thin films of the semiconductors were spin-coated from $CHCl_3$ solution (10 mg/mL, 3000 r/min, 40-60 nm) onto SiO_2 /Si wafers modified with octadecyltrichlorosilane (OTS). All the devices were annealed in a vacuum drying oven to eliminate air and moisture and obtain optimized morphology.

Devices fabrication: The SiO_2/Si wafers used here were cleaned with deionized water, piranha solution (H_2SO_4/H_2O_2=2:1), deionized water, isopropyl alcohol, and finally were blown dry with high-purity nitrogen gas. Treatment of the SiO_2/Si wafers with octadecyltrichlorosilane (OTS) was conducted by the vapor-deposition method. The clean wafers were dried under vacuum at 90 ℃ for 2 h to eliminate the moisture. When the temperature is reduced to approximately room temperature, a small drop of OTS was dropped onto the wafers. Subsequently, this system was heated to 120 ℃ for 2 h under vacuum, after which the vacuum is maintained at approximately room temperature.

The traditional bottom-gate bottom-contact (BGBC) devices based on the thin films were spin-coated on the OTS/SiO_2/Si wafers containing lithographic Au as source and drain electrodes. All electrical characteristics of the devices were measured at room temperature using a semiconductor parameter analyser (Keithley 4200 SCS) and Micromanipulator 6150 probe station. The mobility of the devices were calculated in the saturation regime. The equation is listed as follows:

$$I_{DS}=(W/2L)C_i\mu(V_{GS}-V_T)^2$$

where W/L is the channel width/length, C_i is the insulator capacitance per unit area, and V_{GS} and V_T are the gate voltage and threshold voltage, respectively.

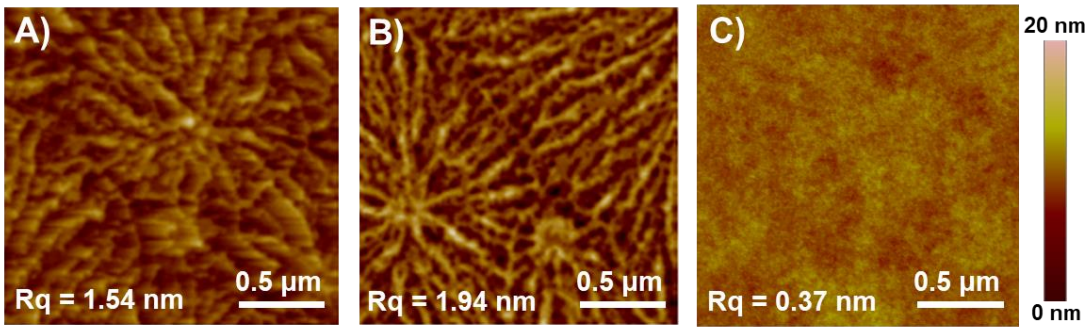

Figure S2. AFM images of thin films annealed at different temperatures. A) **P-1** at 120 ℃, B) **P-2** at 160 ℃ and C) **P-3** at 160 ℃.

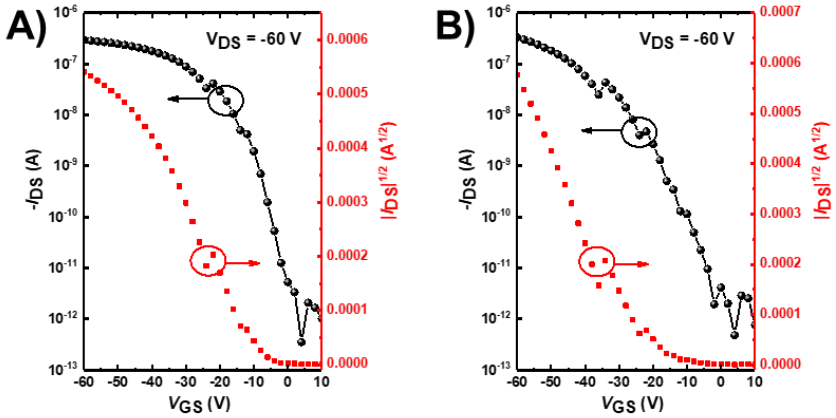

Figure S3. Transfer curves of the thin film transistors annealed at different temperatures: A) **P-1** at 120 ℃, B) **P-2** at 160 ℃.

Table S2. OFET Device Parameters.

Comps.	W/L (μm)	Temp. (°C)	μ_{ave} ($cm^2 V^{-1} s^{-1}$)	μ_{max} ($cm^2 V^{-1} s^{-1}$)	V_t (V)	On/off Ratio
P-1	1400/20	120	2.2×10^{-4}	4.3×10^{-4}	-6.6	8.3×10^{5}
P-2	1400/20	160	3.5×10^{-4}	6.3×10^{-4}	-21.7	6.9×10^{5}
P-3	1400/50	160	2.5×10^{-5}	3.5×10^{-5}	-7.8	1.0×10^{4}

5. OLED fabrication and characterization

The substrates were ultrasonic cleaned with deionized water and anhydrous ethanol consecutively, and then dried with nitrogen gas. Then the substrates were treated with ultraviolet ozone for 15 minutes to remove surface contaminants. Then PEDOT: PSS aqueous solution (Clevios P VP AI 4083) was spin-coated on the substrates at 3000 rpm for 30 s to form a ~25 nm film, followed by annealing at 150 ℃ for 15 min. After that, the substrates were transferred to the nitrogen glove box for subsequent operation. PVK and emission materials were mixed (16:1，w/w) and dissolved in chlorobenzene. The mixed solutions were then spin-coated on the substrates at 3000 rpm for 30 s and baked at 150 ℃ for 10min. After that, the devices were transferred into the vacuum chamber for depositing 40 nm TPBI, 20 nm Ca and 80 nm Al cathode.

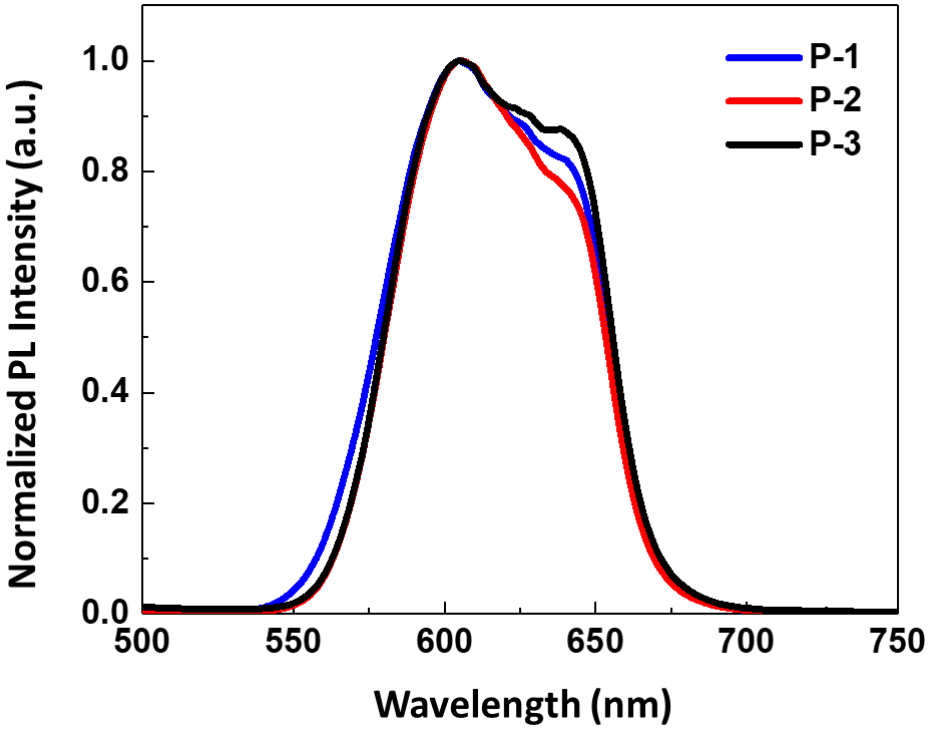

Figure S4. The PL spectra of the blend emission layer on quartz

6. References.

1. L. Lv, J. Roberts, C. Xiao, Z. Jia, W. Jiang, G. Zhang, C. Risko and L. Zhang, *Chem. Sci.*, 2019, 10, 4951–4958.

7. ^{1}H NMR, ^{13}C NMR and HRMS Spectra of compounds

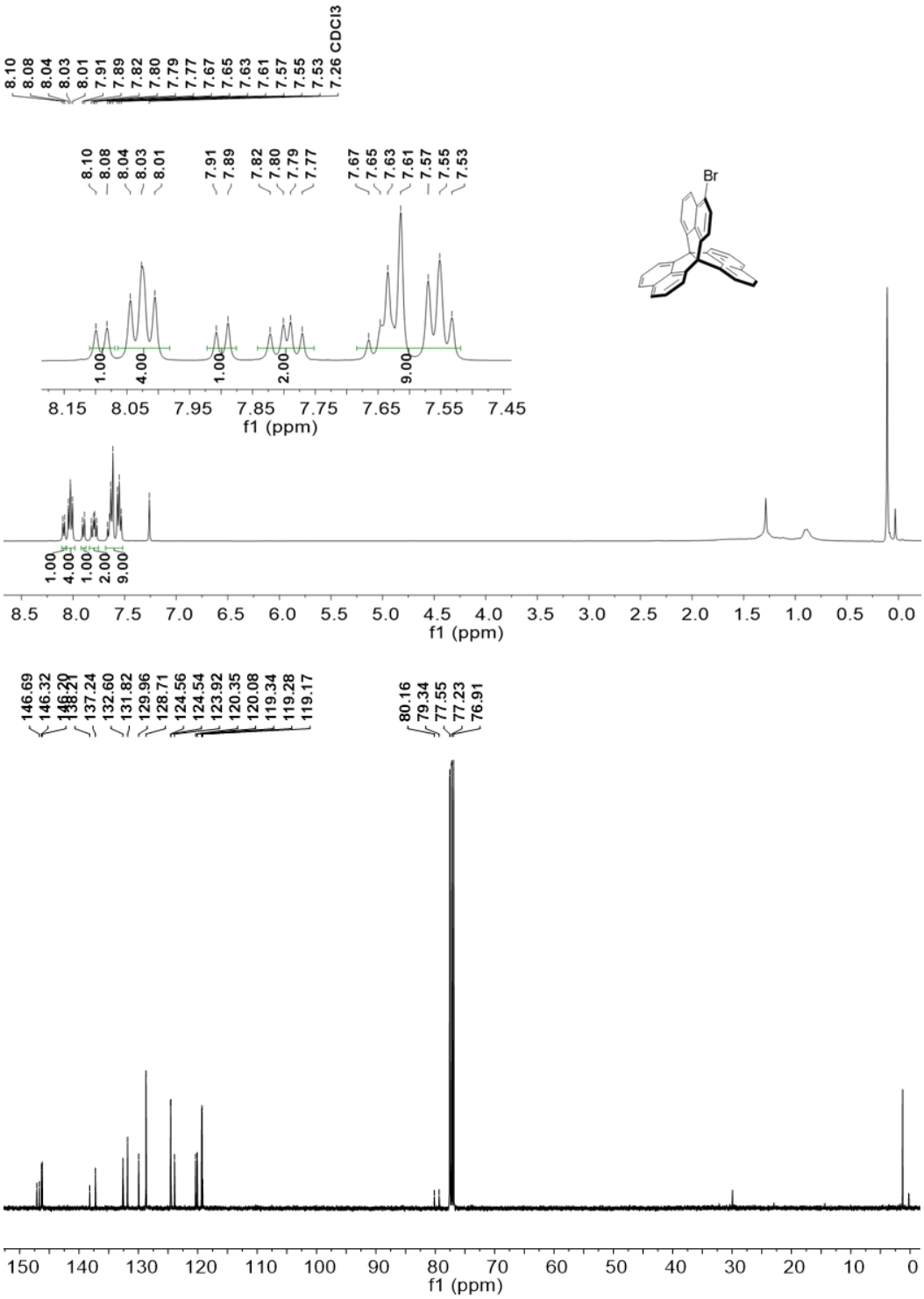

Figure S5. ^{1}H NMR (top) and ^{13}C NMR (bottom) of **2.** (^{1}H NMR and ^{13}C NMR in $CDCl_3$ at 300 K)

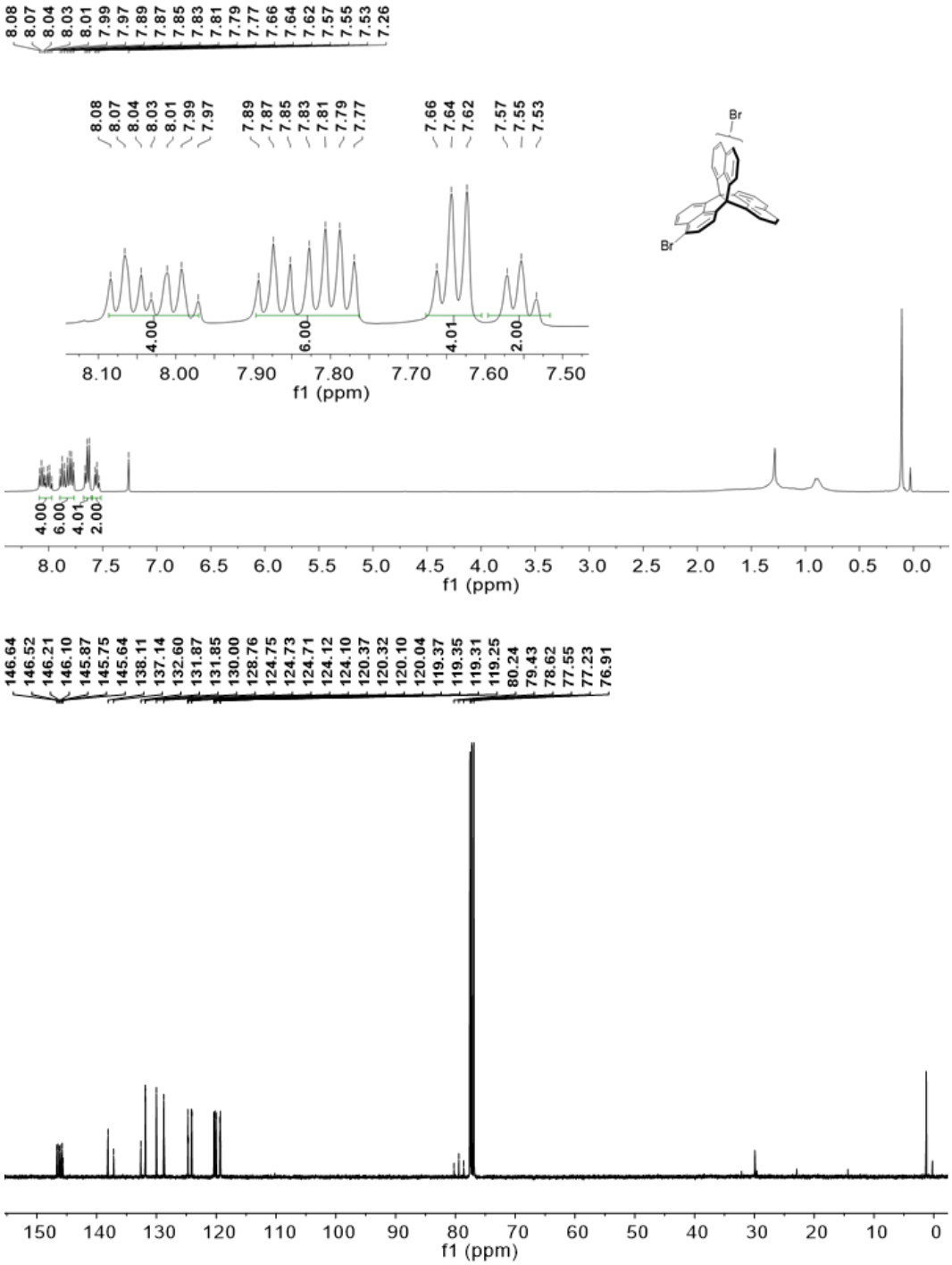

Figure S6. ^{1}H NMR (top) and ^{13}C NMR (bottom) of **3.** (^{1}H NMR and ^{13}C NMR in $CDCl_3$ at 300 K).

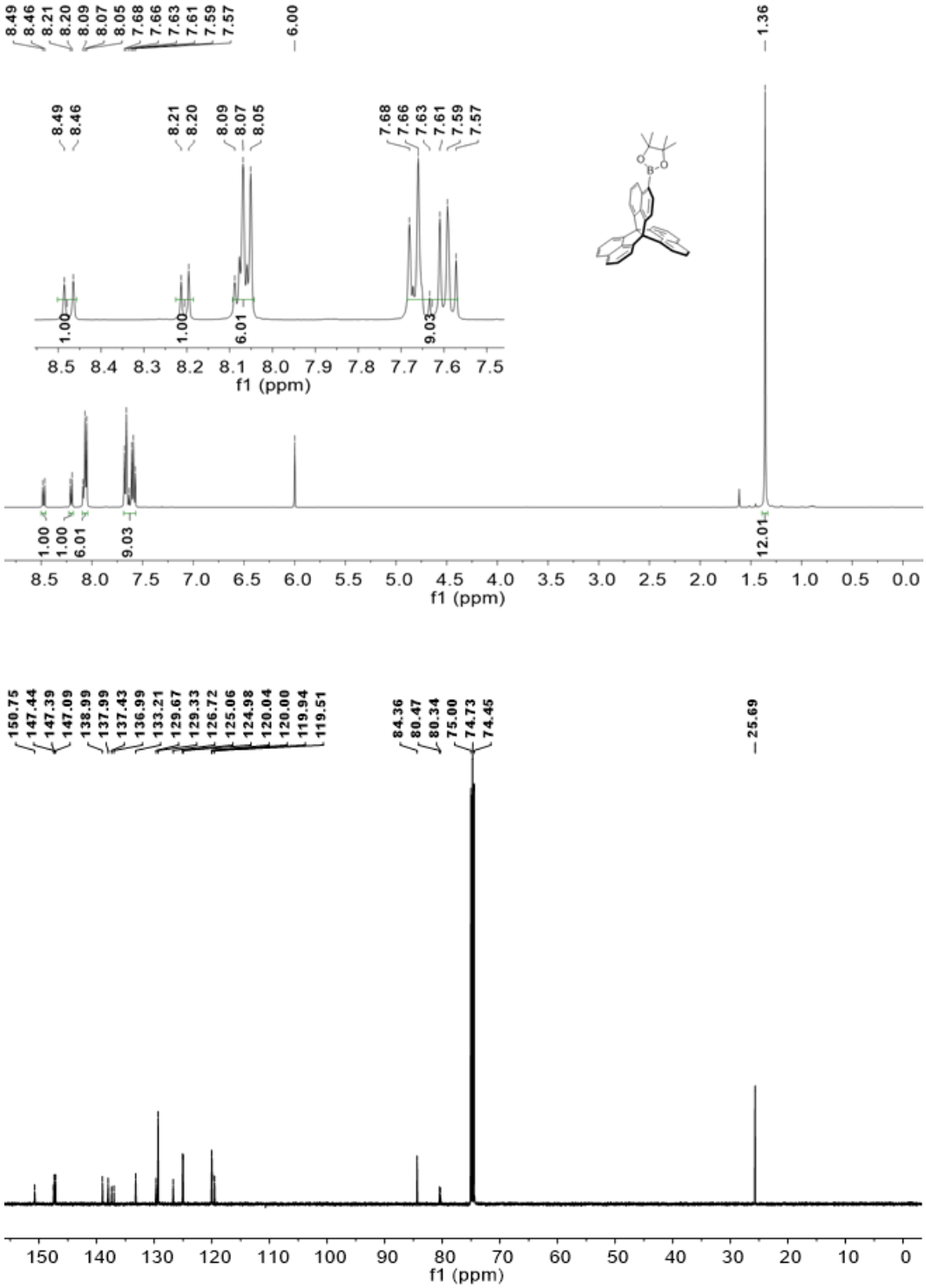

Figure S7. ^{1}H NMR (top) and ^{13}C NMR (bottom) of **4.** (^{1}H NMR and ^{13}C NMR in $C_2D_2Cl_4$ at 373 K)

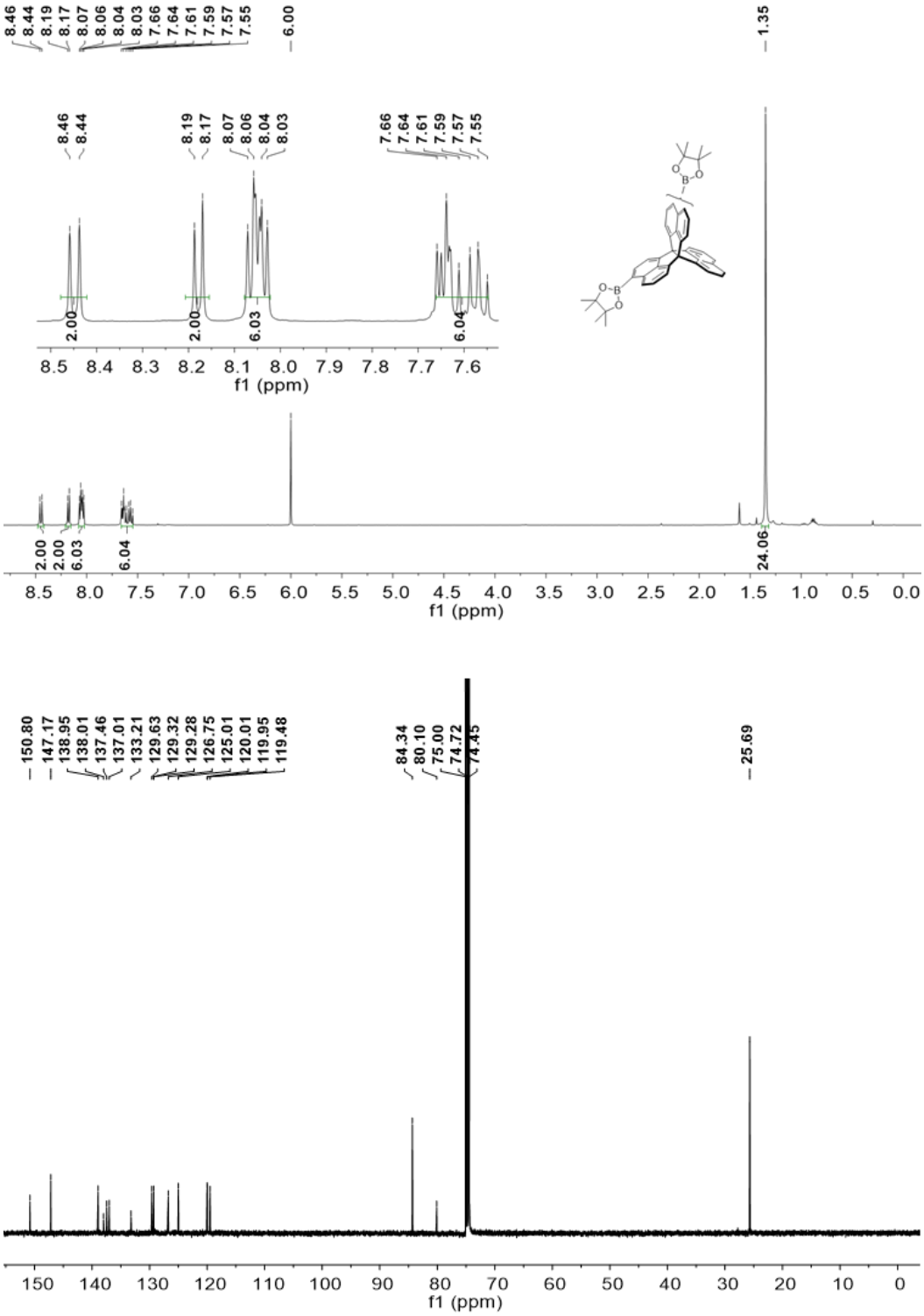

Figure S8. ^{1}H NMR (top) and ^{13}C NMR (bottom) of **5.** (^{1}H NMR and ^{13}C NMR in $C_2D_2Cl_4$ at 373 K)

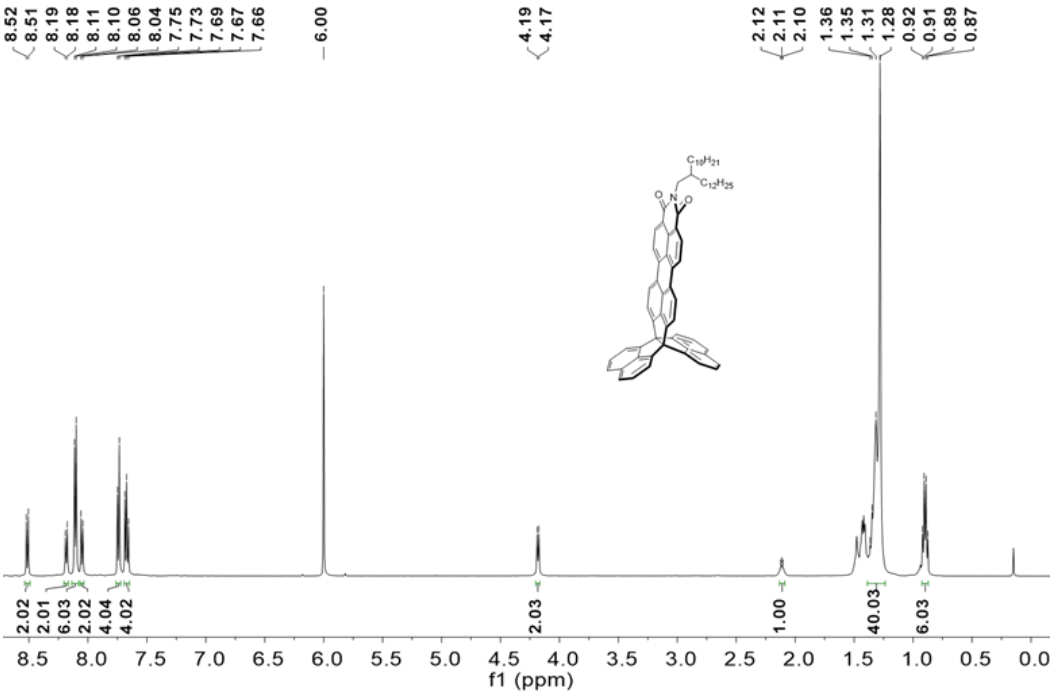

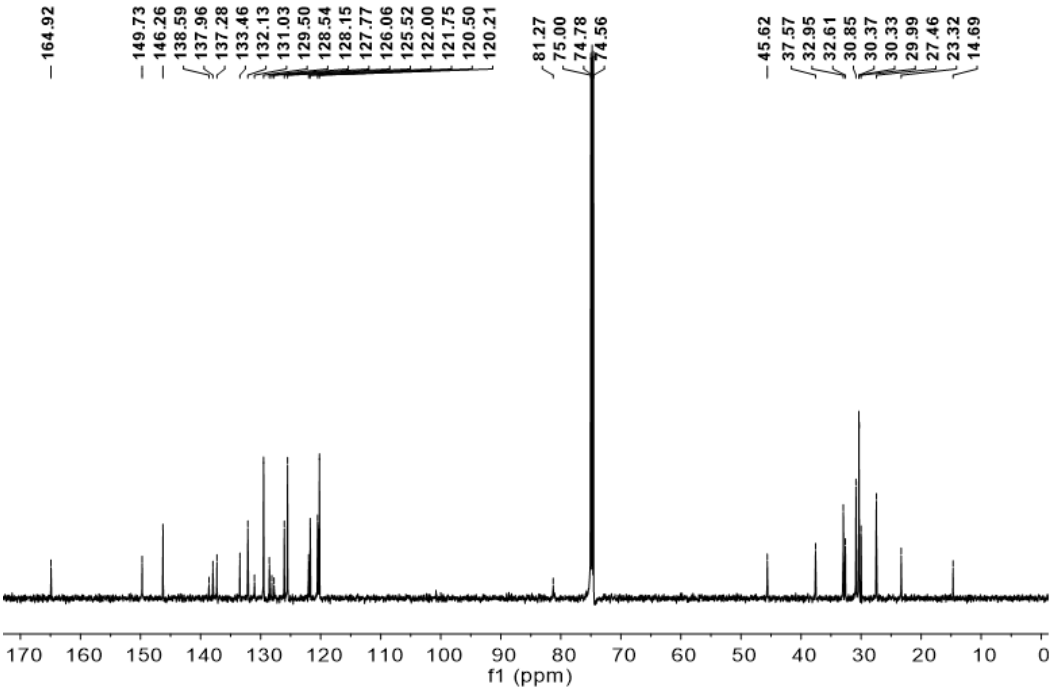

Figure S9. ^{1}H NMR (top) and ^{13}C NMR (bottom) of **P-1** (^{1}H NMR and ^{13}C NMR in $C_2D_2Cl_4$ at 373 K).

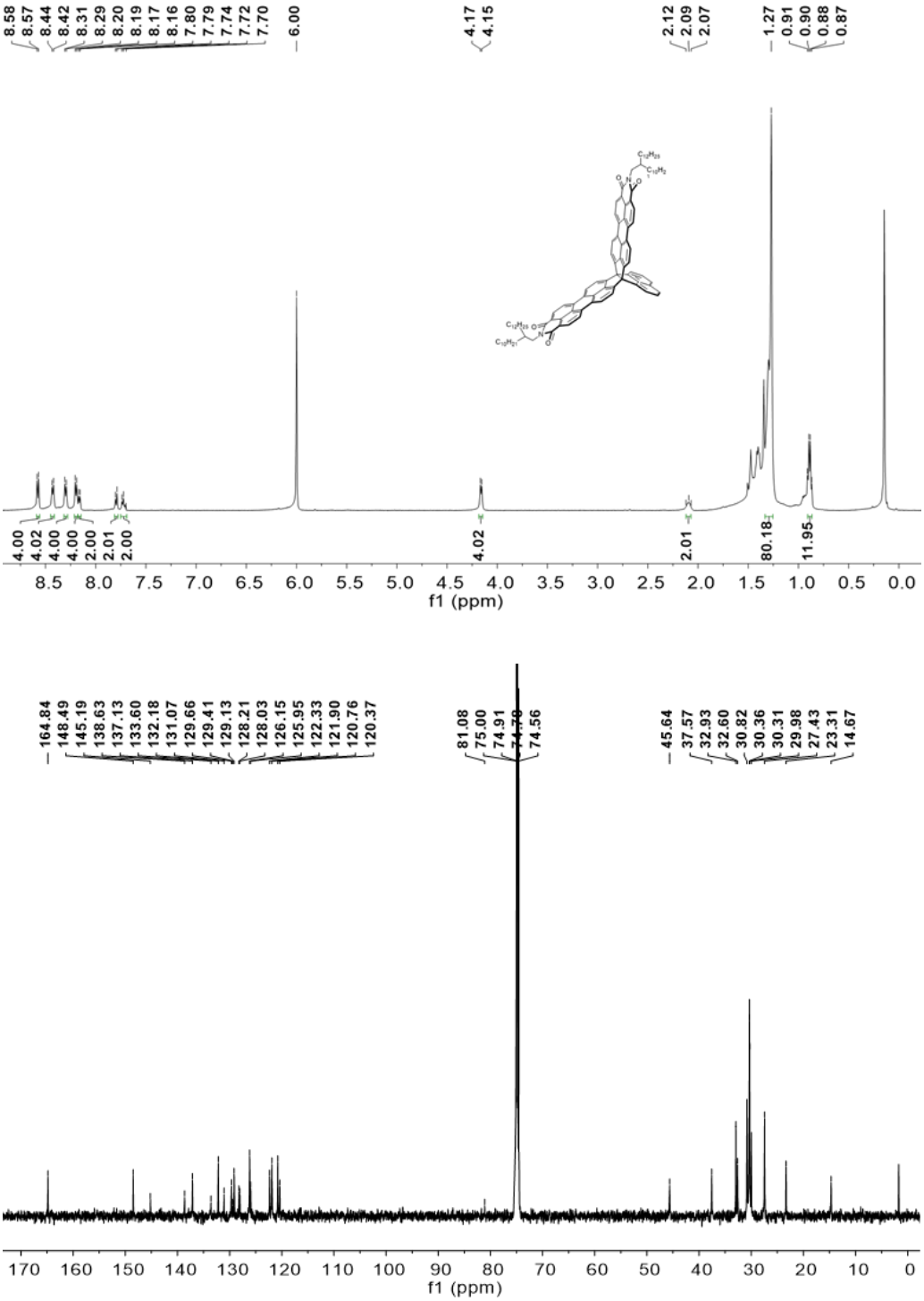

Figure S10. ^{1}H NMR (top) and ^{13}C NMR (bottom) of **P-2** (^{1}H NMR and ^{13}C NMR in $C_2D_2Cl_4$ at 373 K).

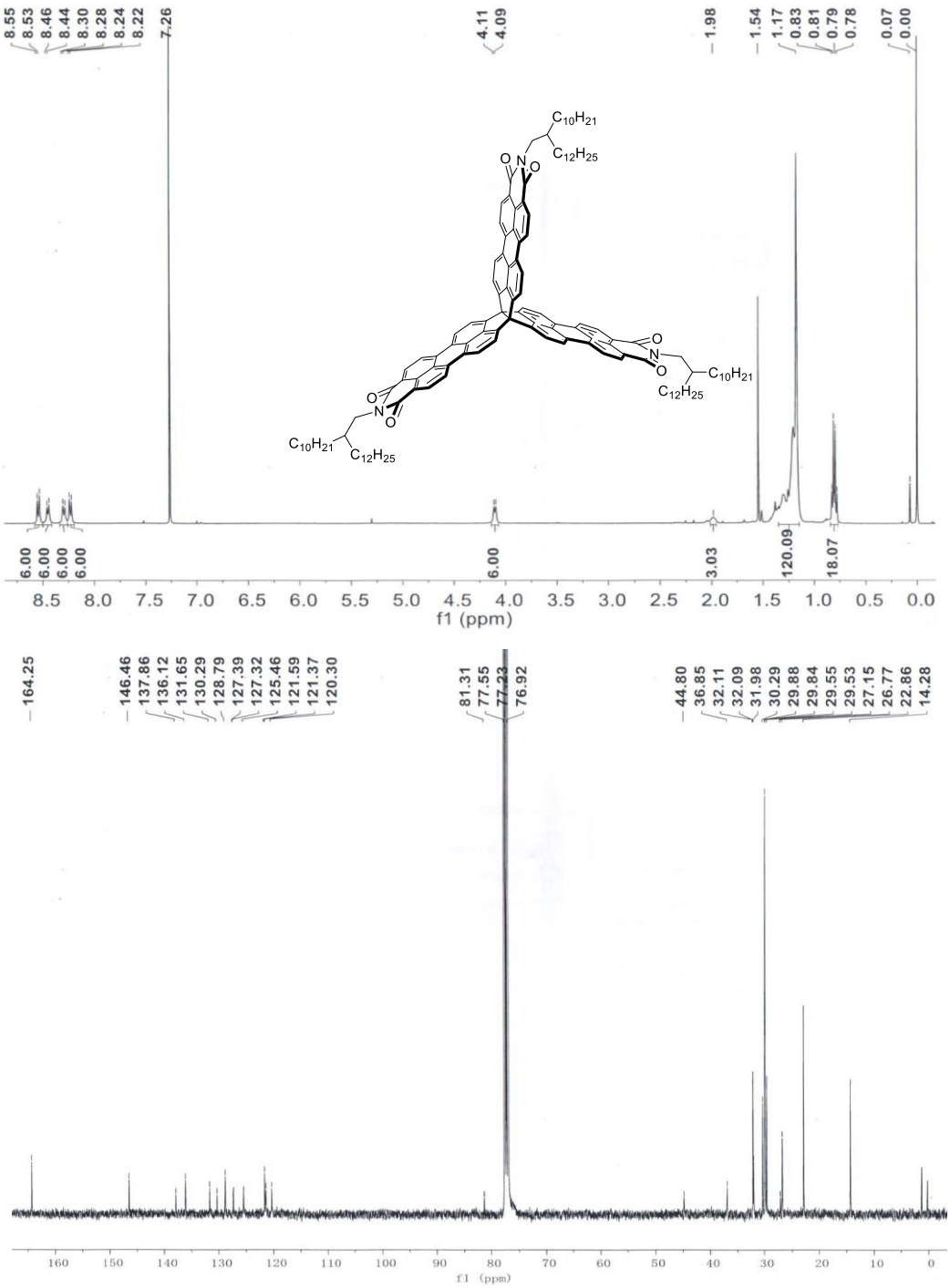

Figure S11. ^{1}H NMR (top) and ^{13}C NMR (bottom) of **P-3** (^{1}H NMR and ^{13}C NMR in $CDCl_3$ at 300 K).

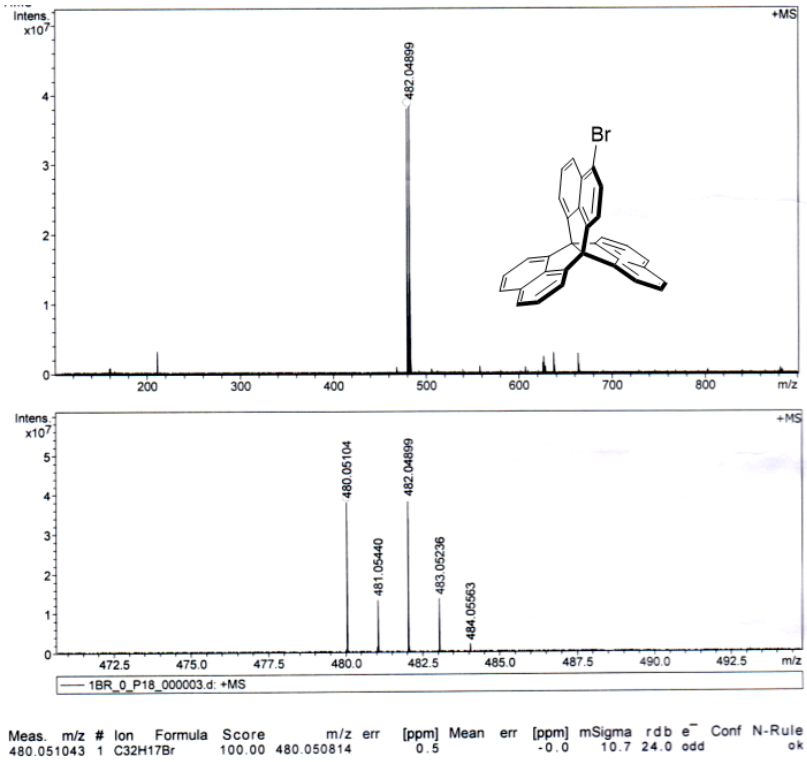

Figure S12. HR-MALDI-TOF spectra of **2**.

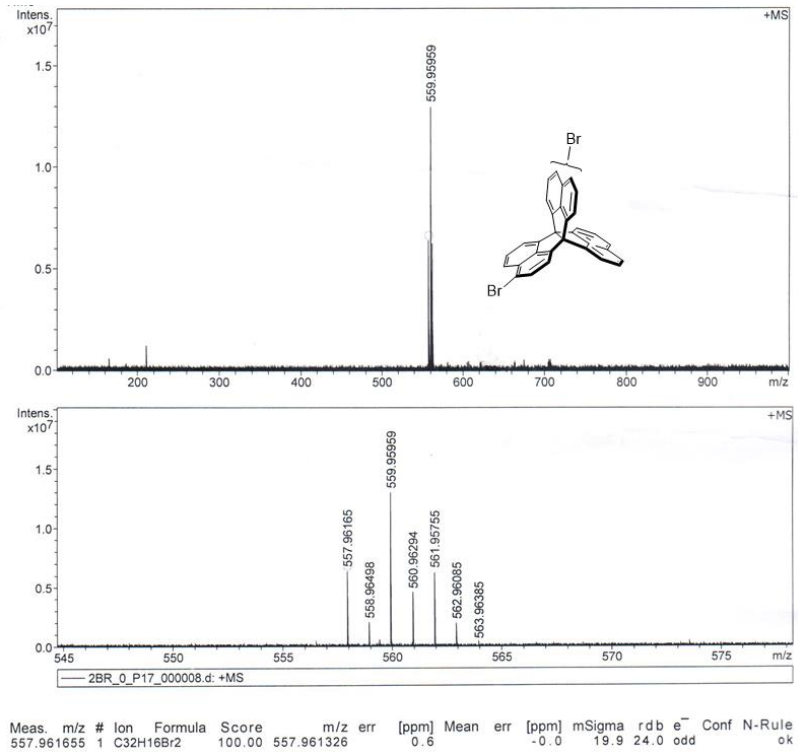

Figure S13. HR-MALDI-TOF spectra of **3**.

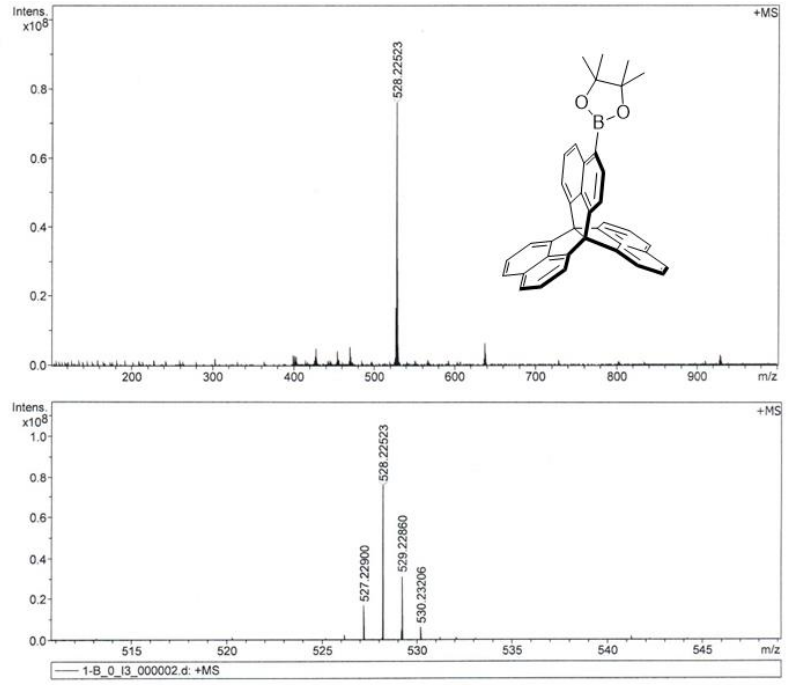

Meas. m/z	#	Ion Formula	Score	m/z	err [ppm]	Mean err [ppm]	mSigma	rdb	e⁻ Conf	N-Rule
528.225227	1	C38H29BO2	100.00	528.226167	1.8	1.4	7.5	25.0	odd	ok

Figure S14. HR-MALDI-TOF spectra of **4**.

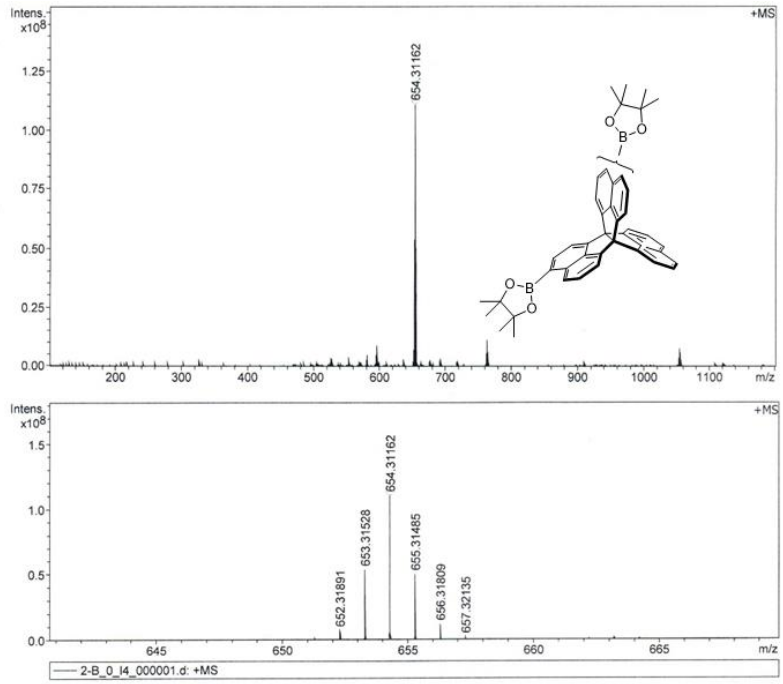

Meas. m/z	#	Ion Formula	Score	m/z	err [ppm]	Mean err [ppm]	mSigma	rdb	e⁻ Conf	N-Rule
654.311619	1	C44H40B2O4	100.00	654.312153	-1.4	0.2	26.1	26.0	odd	ok

Figure S15. HR-MALDI-TOF spectra of **5**.

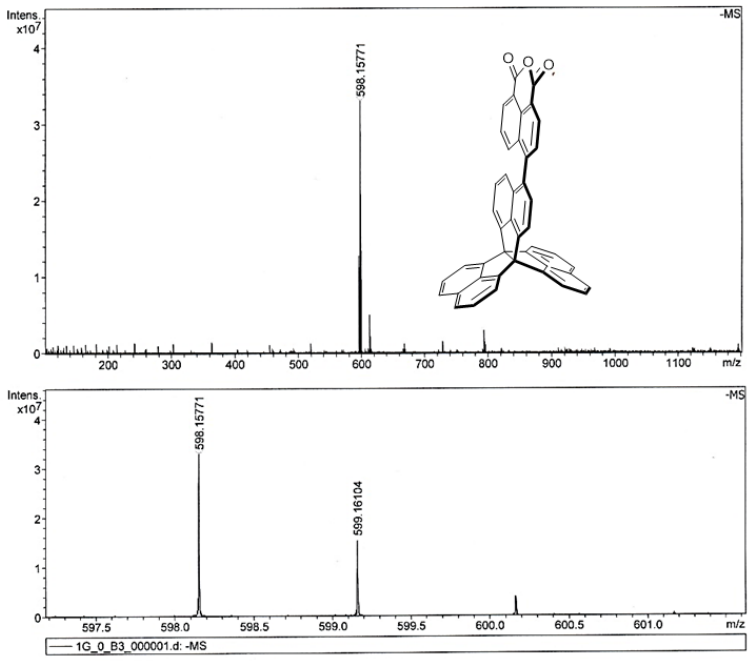

Meas. m/z	#	Ion Formula	Score	m/z	err [ppm]	Mean err [ppm]	mSigma	rdb	e⁻ Conf	N-Rule
598.157714	1	C44H22O3	100.00	598.157443	0.5	-0.4	6.3	34.0	odd	ok

Figure S16. HR-MALDI-TOF spectra of **6**.

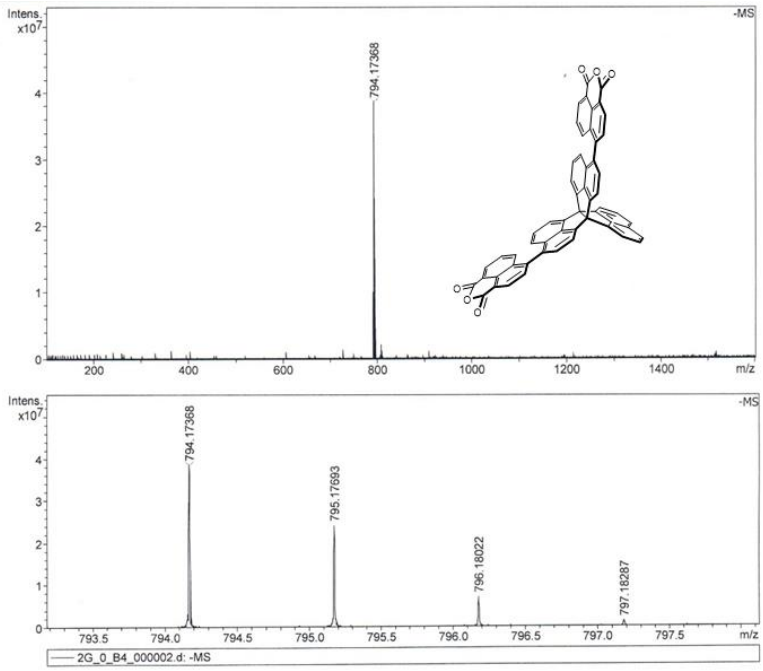

Meas. m/z	#	Ion Formula	Score	m/z	err [ppm]	Mean err [ppm]	mSigma	rdb	e⁻ Conf	N-Rule
794.173684	1	C56H26O6	100.00	794.173487	-0.2	-0.2	9.0	44.0	odd	ok

Figure S17. HR-MALDI-TOF spectra of **7**.

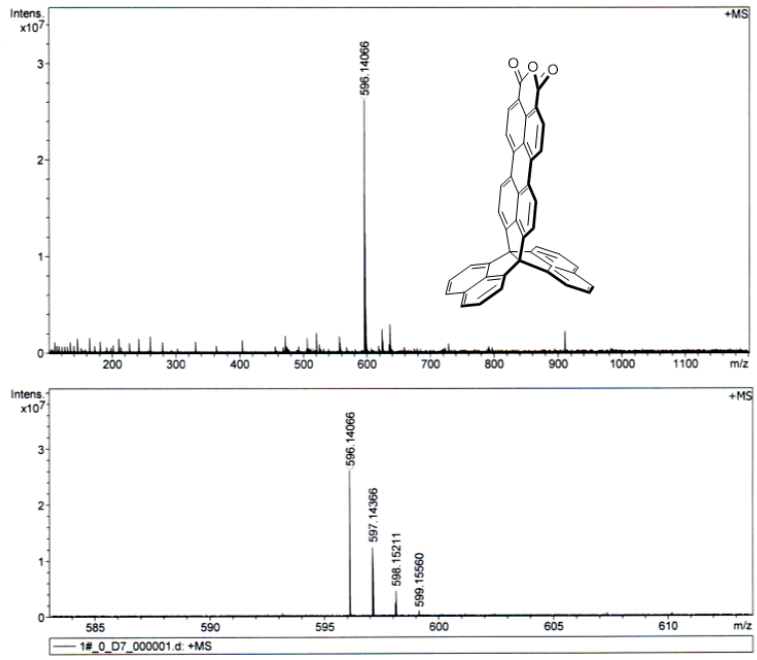

Meas. m/z	#	Ion Formula	Score	m/z	err [ppm]	Mean err [ppm]	mSigma	rdb	e⁻ Conf	N-Rule
596.140664	1	C44H20O3	100.00	596.140696	0.1	0.3	11.2	35.0	odd	ok

Figure S18. HR-MALDI-TOF spectra of **8**.

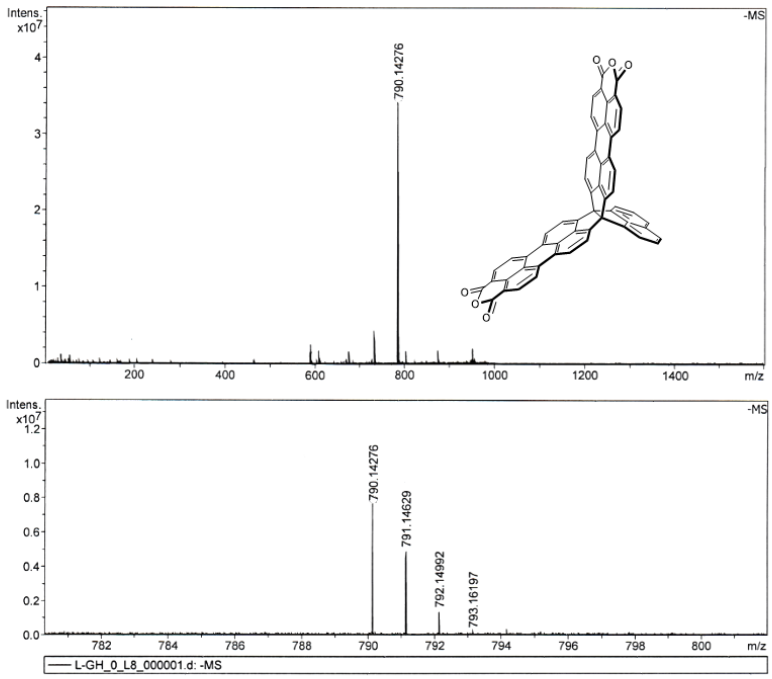

Meas. m/z	#	Ion Formula	Score	m/z	err [ppm]	Mean err [ppm]	mSigma	rdb	e⁻ Conf	N-Rule
790.142763	1	C56H22O6	100.00	790.142187	0.7	-0.9	24.3	46.0	odd	ok

Figure S19. HR-MALDI-TOF spectra of **9**.

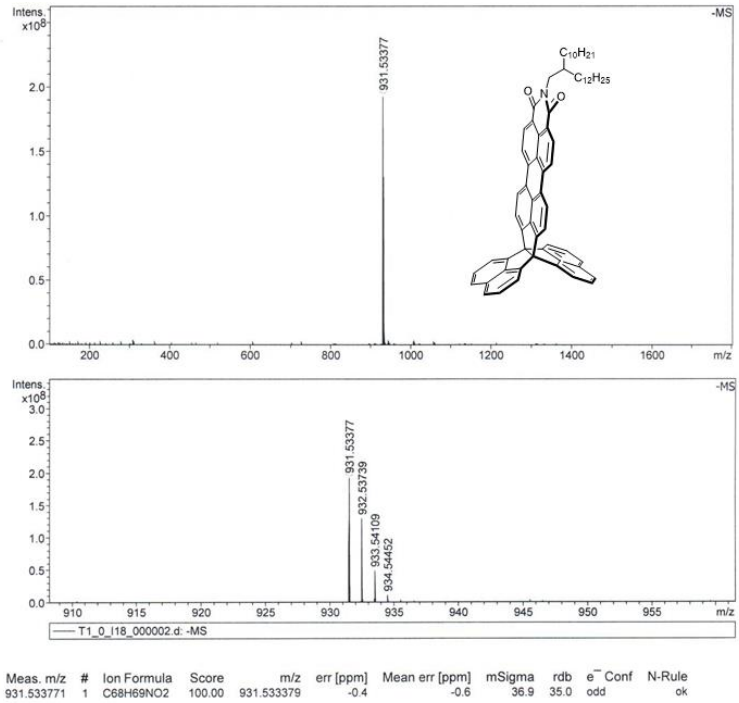

Figure S20. HR-MALDI-TOF spectra of **P-1**.

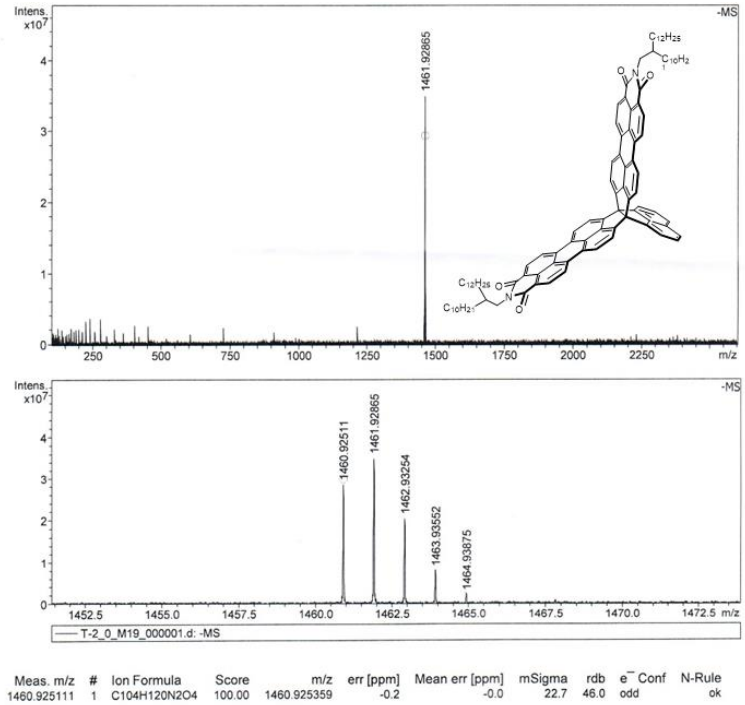

Figure S21. HR-MALDI-TOF spectra of **P-2**.

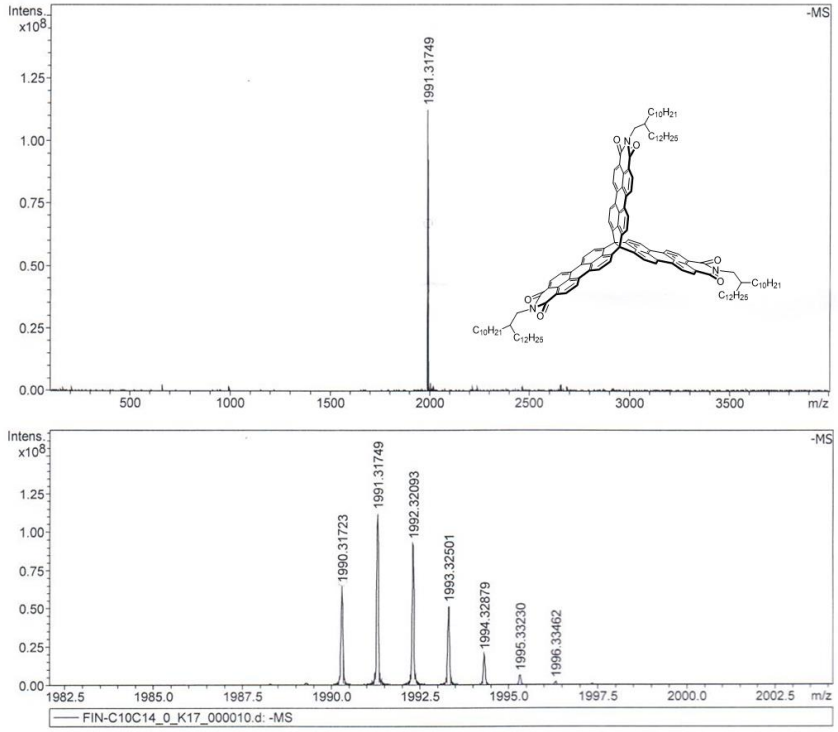

Meas. m/z	#	Ion Formula	Score	m/z	err [ppm]	mSigma	rdb	e⁻ Conf	N-Rule
1990.317230	1	C140H171N3O6	100.00	1990.317339	0.1	40.8	57.0	odd	ok

Figure S22. HR-MALDI-TOF spectra of **P-3**.